Published in final edited form as:
*Vis Neurosci*. 2000 ; 17(5): 667–678.

# Rod and cone visual cycle consequences of a null mutation in the 11-*cis*-retinol dehydrogenase gene in man

**ARTUR V. CIDECIYAN**[1,*], **FRANÇOISE HAESELEER**[2,*], **ROBERT N. FARISS**[2], **TOMAS S. ALEMAN**[1], **GEENG-FU JANG**[2], **CHRISTOPHE L. M. J. VERLINDE**[5], **MICHAEL F. MARMOR**[6], **SAMUEL G. JACOBSON**[1], and **KRZYSZTOF PALCZEWSKI**[2,3,4]

1*Department of Ophthalmology, Scheie Eye Institute, University of Pennsylvania, Philadelphia*

2*Department of Ophthalmology, University of Washington, Seattle*

3*Department of Chemistry, University of Washington, Seattle*

4*Department of Pharmacology, University of Washington, Seattle*

5*Biological Structure and BioMolecular Structure Center, University of Washington, Seattle*

6*Department of Ophthalmology, Stanford University, Stanford*

## Abstract

Vertebrate vision starts with photoisomerization of the 11-*cis*-retinal chromophore to all-*trans*-retinal. Biosynthesis of 11-*cis*-retinal is required to maintain vision. A key enzyme catalyzing the oxidation of 11-*cis*-retinol is 11-*cis*-retinol dehydrogenase (11-*cis*-RDH), which is encoded by the *RDH5* gene. 11-*cis*-RDH is expressed in the RPE and not in the neural retina. The consequences of a lack of 11-*cis*-RDH were studied in a family with fundus albipunctatus. We identified the causative novel *RDH5* mutation, Arg157Trp, that replaces an amino acid residue conserved among short-chain alcohol dehydrogenases. Three-dimensional structure modeling and *in vitro* experiments suggested that this mutation destabilizes proper folding and inactivates the enzyme. Studies using RPE membranes indicated the existence of an alternative oxidizing system for the production of 11-*cis*-retinal. *In vivo* visual consequences of this null mutation showed complex kinetics of dark adaptation. Rod and cone resensitization was extremely delayed following full bleaches; unexpectedly, the rate of cone recovery was slower than rods. Cones showed a biphasic recovery with an initial rapid component and an elevated final threshold. Other unanticipated results included normal rod recovery following 0.5% bleach and abnormal recovery following bleaches in the 2–12% range. These intermediate bleaches showed rapid partial recovery of rods with transitory plateaux. Pathways in addition to 11-*cis*-RDH likely provide 11-*cis*-retinal for rods and cones and can maintain normal kinetics of visual recovery but only under certain constraints and less efficiently for cone than rod function.

### Keywords

Cone; Fundus albipunctatus; Phototransduction; RPE; Rod

## Introduction

Vision begins in the vertebrate retina when a photon is absorbed by 11-*cis*-retinal, the chromophore of rod and cone photoreceptor visual pigments, causing isomerization to all-

Address correspondence and reprint requests to: Artur V. Cideciyan, Scheie Eye Institute, University of Pennsylvania, 51 N. 39th Street, Philadelphia, PA 19104, USA. E-mail: cideciya@mail.med.upenn.edu.
*Contributed equally to this work.

*trans*-retinal (Palczewski & Saari, 1997). Critical to vision is the removal of the photolyzed chromophore and recombination of opsin and 11-*cis*-retinal to allow regeneration of visual pigments, and continuation of visual perception. In addition to photoreceptors, the visual cycle is believed to involve adjacent retinal pigment epithelial cells (RPE) (Bok, 1993). There are also suggestions that retinal cells other than photoreceptors participate in this process (Bunt-Milam & Saari, 1983; Das et al., 1992; Jin et al., 1994; Crouch et al., 1996).

Despite considerable progress, current understanding of the molecular mechanisms of the visual cycle in man is incomplete. One way to gain insight is to analyze the consequences to human vision of mutations in genes implicated in the visual cycle. Recently, a retinopathy called fundus albipunctatus was associated with mutations in *RDH5* (Yamamoto et al., 1999; Gonzalez-Fernandez et al., 1999), the gene that encodes NAD0NADP-dependent 11-*cis*-retinol dehydrogenase (11-*cis*-RDH) (Lion et al., 1975; Simon et al., 1995). 11-*cis*-RDH belongs to a short-chain alcohol dehydrogenase superfamily of enzymes that catalyze oxidation/reduction of hydrophobic substrates, including retinoids and steroids (Jornvall et al., 1995). 11-*cis*-RDH is proposed to catalyze oxidation of 11-*cis*-retinol to 11-*cis*-retinal in the RPE, while in other tissues it might be involved in oxidation of 9-*cis*-retinol or steroids (Driessen et al., 1998). To date, two *RDH5* mutations have been analyzed biochemically and show significantly reduced but detectable enzymatic activity (Yamamoto et al., 1999). Detailed analyses of the relationships between genotype and visual cycle defect have not been reported.

The aim of the present work was to explore the consequences to the human visual cycle of abnormal 11-*cis*-RDH activity. We identified a family with fundus albipunctatus harboring a novel *RDH5* mutation. Biochemical and structural analyses indicated a complete lack of activity of the mutant enzyme. An additional NADP/NADPH-specific red-ox system in bovine RPE microsomes was found. *In vivo* studies of vision in a homozygote indicated that lack of 11-*cis*-RDH activity has highly selective effects on the visual cycle and causes more cone than rod dysfunction. Our results imply that in man there are multiple oxidation pathways for 11-*cis*-retinal production following a flash-bleach and the dominant pathway may be determined by the extent of the bleach.

## Methods

### Mutation analysis

The four coding exons for the *RDH5* gene were amplified by PCR from genomic DNA using intronic primers (Yamamoto et al., 1999). Each exon was directly sequenced in both directions using the BigDye Terminator Cycle Sequencing Kit (Applied Biosystems, La Jolla, CA).

### Expression of Arg157Trp mutant of 11-cis-RDH in insect cells

Human wild-type (wt) 11-*cis*-RDH was produced in insect SF9 cells as described previously (Saari et al., 2000). The Arg157Trp mutant was recreated by replacing a fragment *NcoI-BclI* from the cloned wt 11-*cis*-RDH with a fragment *NcoI-BclI* from the mutated exon 3, and a six His tag sequence was added by PCR to the C-terminus. All PCR products were cloned in pCRII-TOPO vector and sequenced. The coding sequences of human 11-*cis*-RDH and Arg157Trp mutant were then cloned in the pFastBac1 expression vector before transferring it to Bac-To-Bac baculovirus expression system (Life Technologies, Inc., La Jolla, CA).

### Preparation of [$^3$H]pro-S-NADH and [$^3$H]pro-S-NADPH

L-Glutamate dehydrogenase (400 μl, Sigma/Aldrich, La Jolla, CA) was mixed with 0.25 mCi of L-[2,3-$^3$H]-glutamic acid (Dupont New England Nuclear, Boston, MA; 24 Ci/mmol), in 10 mM BTP, pH 7.4 containing 50 mM NaCl, 5 mM L-glutamic acid, 1 mM ADP, 10 mM β-NAD, or 10 mM β-NADP. The reaction was carried out overnight in the dark at room

temperature. Dinucleotides were purified on a Mono Q HR 505 column (Pharmacia, Freiburg, Germany) equilibrated with 10 mM BTP, pH 7.3, using 0–500 mM NaCl.

### Measurement of 11-cis-RDH activity

RDH activity was measured by following the transfer of [$^3$H] from [$^3$H]-NADPH (150,000 dpm/nmol) or from [$^3$H]-NADH (150,000 dpm/nmol) to 11-*cis*-retinal. Detailed description of the assay was published previously (Saari et al., 1993). Briefly, insect cells were harvested 74 h after infection with recombinant baculovirus. The cells were homogenized in water and centrifuged at 16,000*g* for 5 min. The pellet was resuspended in water three times the volume of the pellet. Membranes (1–20 μl) were used in the reaction mixture composed of 50 mM 2-(N-morpholino)ethanesulfonic acid (MES), pH 5.5, containing 10–50 μM [$^3$H]-labeled dinucleotides and 60 μM 11-*cis*-retinol. The reaction is quenched with 400 μl of methanol, 50 μl of 100 mM $NH_2OH$, and 50 μl of 1 M NaCl. The retinoids were extracted with hexane (500 μl). The samples were shaken for 3 min and the phases were separated by centrifugation for 3 min at 16,000*g*. Radioactivity was measured in 250 μl of the organic phase. Similar assay was performed to determine the 11-*cis*-RDH activity in RPE microsomes isolated from bovine eyes (Saari & Bredberg, 1990). The assay is ~25–50 times more sensitive than more traditional HPLC analysis.

### Preparation of anti-11-cis-RDH polyclonal antibodies and immunolocalization

Rabbit anti-11-*cis*-RDH polyclonal antibodies (UW40 and UW41) were raised against a peptide from the catalytic domain of 11-*cis*-RDH, SKFGLEAFSDSLRRDV, coupled to a carrier protein as described previously (Palczewski et al., 1993). Cryosections of retinal tissue from monkeys (*Macaca nemestrina*), fixed in 4% formaldehyde (Otto-Bruc et al., 1997), were incubated overnight with UW40 or UW41 diluted 1:1000 in phosphate buffered saline (pH 7.2) containing bovine serum albumin (0.5%), Triton X-100 (0.05%), and sodium azide (0.05%). After repeated washing, sections were incubated 2 h in goat anti-rabbit Cy3 (Jackson Immuno-Research, Mississauga, Canada) washed, and analyzed on a BioRad 600 confocal microscope (WM Keck Center for Advanced Studies in Neural Signaling at the University of Washington).

### Model of 11-cis-RDH

From a FASTA search (Pearson & Lipman, 1988) in the Protein DataBank (PDB), 17-β-hydroxysteroid dehydrogenase [PDB entry: 1FDT at 2.2 ° resolution (Breton et al., 1996)] was identified as the three-dimensional structure with the highest sequence similarity to 11-*cis*-RDH. Subsequently, a model was constructed with the HOMOLOGY module of the INSIGHTII software (Molecular Simulations, Inc., La Jolla, CA) using established homology modeling protocols (Ring & Cohen, 1993).

### Human studies

The proband (age 57) and his brother (age 61) from a family with fundus albipunctatus (Marmor, 1977, 1990) underwent a complete clinical evaluation and a series of psychophysical and electrophysiological tests. Best corrected acuities were 20/20 for both patients. The proband had spherical equivalent of −0.50, right eye and −1.75, left eye; the brother had no refractive error. There were minimal nuclear sclerotic lens changes in both subjects. Goldmann kinetic perimetry (V4e, I4e) and standard electroretinograms were within normal limits. There were no coexisting systemic abnormalities or intake of retinotoxic medication. Fundus appearance of the proband was typical for fundus albipunctatus (Marmor, 1977, 1990) and that of his brother was normal except for rare white dots. Research procedures were in accordance with institutional guidelines and the Declaration of Helsinki.

### Psychophysics

Dark- and light-adapted static threshold perimetry, bleaching, and background adaptation were performed (Jacobson et al., 1986). All stimuli were 1.7 deg in diameter and 200 ms in duration; pupils were fully dilated. For perimetry, thresholds were measured in the dark-adapted state with 500- and 650-nm stimuli; long- and middle-wavelength sensitive cone (L/M-cone) thresholds were measured with 600 nm on a 2.7 log phot-td white background; and short-wavelength sensitive cone (S-cone) thresholds were measured with 440 nm on a 3.4 log phot-td yellow background. For bleaching adaptation, 500- and 650-nm stimuli were used at a locus 12 deg in the inferior field (Cideciyan et al., 1997, 1998). Flashes estimated to isomerize 0.5%, 2%, 3.5%, 6%, 12%, and 97% of rhodopsin were presented and thresholds determined until prebleach values were attained. At key periods during recovery, thresholds to 420-, 440-, 480-, or 540-nm stimuli were also determined (Cideciyan et al., 1997). Two additional loci (6 deg nasal and 30 deg superior field) were also tested with the 97% bleach. For background adaptation, thresholds were measured at 12 deg inferior field dark adapted or on an achromatic background which varied over −3.3 to +2.7 log scot-td range. Thresholds for 500 and 650 nm were determined alternately at each background to allow identification of the rod or cone mechanism mediating detection (Cideciyan et al., 1998). Rod and cone background adaptation functions were fit to the following mathematical model:

$$\log T = \log T_0 + \log\left[\left(A + A_0\right) / A_0\right]^n,$$

where log $T$ is the threshold, $A$ is the background, log $T_0$ and log $A_0$ specify the vertical and horizontal positions of the function on log–log coordinates, and $n$ is the slope of the diagonal line (Hood & Greenstein, 1990).

### Electroretinography (ERG)

ERG photoresponses were recorded using a red (Kodak Wratten 26) and two blue (W47A) flash stimuli with equipment and methodology described before (Cideciyan & Jacobson, 1996; Cideciyan et al., 1998; Cideciyan, 2000). The red flash (3.6 log phot-td.s) was photopically matched to the higher energy blue flash (4.6 log scot-td.s) and scotopically matched to the lower energy blue flash (2.3 log scot-td.s). A model of phototransduction consisting of the sum of rod and cone components was used to quantify the dark-adapted waveforms (Cideciyan, 2000). This model has maximum amplitude ($R_{max}$) and sensitivity ($\sigma$) parameters for rod and cone components. Cone-isolated ERG photoresponses were recorded on a rod-desensitizing 3.2 log td white background with red (W26) flash stimuli. The cone phototransduction model was fit to the leading edges of these photoresponses (Cideciyan, 2000). An abbreviated double-flash paradigm (Birch et al., 1995) was used to estimate the kinetics of the rod photoresponse recovery. In this paradigm, the response to a blue probe (4.6 log scot-td.s) presented 30 s after a blue test flash (4.6 log scot-td.s; ~0.5% rhodopsin bleach) allows an estimate of the kinetics of photoresponse recovery (Cideciyan et al., 1998).

## Results

### A novel mutation in the RDH5 gene encoding 11-cis-RDH is associated with fundus albipunctatus

A family with fundus albipunctatus (Marmor, 1977, 1990) was investigated for mutation in the *RDH5* gene. The patient with fundus albipunctatus was found to be homozygous for the Arg157Trp *RDH5* mutation (Fig. 1A). Asymptomatic parents and a brother are heterozygous for the mutation.

Arg157 is highly conserved in the superfamily of short-chain alcohol dehydrogenases suggesting an important function of this residue (Figs. 1B and 1C). Of interest, Ser73 and Gly238 (Yamamoto et al., 1999) localize to regions not conserved among the short-chain

alcohol dehydrogenases (Fig. 1B). To examine the role of Arg157, we created a three-dimensional model of 11-*cis*-RDH on the basis of the crystal structure of 17-β-HSD1 (Figs. 2A and 2B). The sequence alignment (Fig. 2C) shows 32.3% identity in the overlapping region that is 263 amino acids long. Moreover, the model is likely to be reliable in the three-dimensional region of interest since there are no insertions or deletions in loops and other structural elements around Arg157. The model shows that Arg157 is more than 20 ° away from the NADP and substrate-binding sites (Fig. 2A), suggesting that the mutation to Trp is not expected to affect the shape or character of the catalytic site. However, the Arg157 side chain makes two hydrogen bonds to the beginning of residues 243-251 loop that connects the last two secondary structure elements of the Rossman fold. A Trp residue cannot make these hydrogen bonds, possibly preventing the correct loop conformation. In addition, the residues following the Rossman fold are involved in the protein dimer interface. Hence, besides destroying proper monomer folding, the Arg157Trp mutation could also prevent dimer formation, if such dimers are formed for 11-*cis*-RDH.

### 11-cis-RDH is expressed in the RPE

The expression of 11-*cis*-RDH in the eye was determined using rabbit polyclonal antibodies (UW40 and UW41) generated against a KLH-conjugated 16 amino acid long peptide sequence from 11-*cis*-RDH. Both antibodies strongly and specifically immunolabeled RPE in cryosections of monkey retina (Figs. 3A and 3B) and bovine retina (not shown). These results were consistent with previous work (Lion et al., 1975;Zimmerman, 1976;Suzuki et al., 1993;Mata & Tsin, 1998;Simon et al., 1999). Both antibodies did not label the neural retina except a very faint signal seen in the ganglion cell layer (Figs. 3A and 3B). The specificity of UW40 and UW41 immunolabeling was confirmed through peptide-blocking studies in which RPE immunolabeling was abolished by the addition of 20 μg of the 11-*cis*-RDH peptide (SKFGLEAFSDSLRRDV) to the antisera (Fig. 3C). Further, affinity-purified antibody coupled to CNBr-Sepharose bound only one major protein from RPE, and not retina, and that was identified by microsequencing as 11-*cis*-RDH (Palczewski et al., unpublished).

### 11-cis-RDH activity is abolished by the Arg157Trp mutation

The activity of 11-*cis*-RDH was tested by expressing Arg157Trp mutant and wt enzymes in insect cells. Both proteins were expressed to comparably high levels (~4–6% of membrane proteins) as confirmed by immunoblotting (Fig. 4A). The wt enzyme is efficiently solubilized with a detergent while the mutated protein was partially extracted (Fig. 4B), suggesting major structural changes and misfolding of the mutant. Wt enzyme was highly active in the reduction of 11-*cis*-retinal in the presence of both cofactors NADH and NADPH, although NADH is the preferred dinucleotide (Fig. 4C). The $K_M$ for NADH is 4.1 μM when 11-*cis*-retinal is used as a substrate, while $K_M$ for NADPH is > 150 μM. HPLC and UV/Vis spectroscopy of retinoids produced in the assay confirmed the authenticity of the 11-*cis*-retinol product (Fig. 4D). In contrast, no enzymatic activity was detected using membranes containing the mutated enzyme (Fig. 4C). To illustrate this point in typical reaction conditions, usually 4000–5000 dpm were detected for wt enzyme, and 30–60 dpm were found for the mutant and uninfected SF9 membranes. No activity was observed under various conditions including prolonged time courses up to 1 h, use of 10-fold excess of retinoids and NADH over $K_M$, high concentrations of the mutated enzyme, in the membranes (10-fold more than wt enzyme) or purified (data not shown). The Arg157Trp mutation is thus different from other reported *RDH5* mutations, Ser73Phe and Gly238Trp, which show some residual enzymatic activity (Yamamoto et al., 1999).

### Evidence for an alternative red-ox system for 11-cis-retinal production

Recognizing that visual recovery is slowed but not absent in fundus albipunctatus (Carr et al., 1974; Marmor, 1977; Yamamoto et al., 1999), we tested for the presence of other red-ox systems in RPE that would serve as an alternative pathway(s) for 11-*cis*-retinal production. Using bovine RPE microsome preparations, we found that NADH is more efficiently utilized to reduce 11-*cis*-retinal (Fig. 4E). Predictably, when [$^3$H]-NADH was used in the presence of a 20-fold excess of cold NADPH no significant inhibition was observed [Fig. 4F (a and b)]; but a 20-fold excess of cold NADH lowered incorporation of $^3$H to 11-*cis*-retinal, roughly proportional to the dilution factor [Fig. 4F (c)]. When a similar experiment was performed using [$^3$H]-NADPH as a radioactive substrate, NADPH lowered incorporation of $^3$H to 11-*cis*-retinal, roughly proportional to the dilution factor [Fig. 4F (a and b)]. Unexpectedly, NADH, a more potent substrate of 11-*cis*-RDH (Saari et al., 2000), affected the enzymatic activity only modestly [Fig. 4F (c)], rather than complete inhibition of [$^3$H]-11-*cis*-retinol production as expected. These data, and a similar conclusion obtained previously (Saari et al., 2000), strongly suggest that the RPE contains an additional NADP/NADPH-dependent red-ox system that can oxidize 11-*cis*-retinol.

### Rod vision when 11-cis-RDH activity is missing

The *in vivo* consequences to rod visual function of absent 11-*cis*-RDH activity were determined in the homozygote with the Arg157Trp *RDH5* mutation. Rod phototransduction activation was normal. Sensitivity ($\sigma$) of rod-isolated ERG photoresponses (Fig. 5A) was normal ($\sigma$ = 1.3 log scot-td$^{-1}$ ·s$^{-3}$; normal mean ± s.d. = 1.52 ± 0.15 log scot-td$^{-1}$·s$^{-3}$), suggesting that 11-*cis*-RDH activity does not appreciably contribute to the gain of the early activation phase of human rod phototransduction. Maximum amplitude ($R_{max}$) of rod ERG photoresponses was also normal ($R_{max}$ = 355 μV; normal = 456 ± 54 μV); lack of 11-*cis*-RDH activity thus does not preclude normal length rod outer segments. Consistent with these results were normal rod thresholds throughout most of the visual field (not shown). Background adaptation of the rod visual system to dim lights (causing insignificant pigment bleaching) also did not require 11-*cis*-RDH activity: rod-mediated increment thresholds (Fig. 5C) were normal ($T_0$ = 0.9 log; $A_0$ = −3.05 log; $n$ = 0.86; normal values, $T_0$ = 0.66 ± 0.12 log; $A_0$ = −2.86 ± 0.10 log; $n$ = 0.80 ± 0.04).

Bleaching adaptation to strong lights, however, was dramatically abnormal (Fig. 5E), as expected from earlier work (Marmor, 1977,1990). With a full rhodopsin bleach, the cone–rod break was delayed to 120 min (normal = 14 ± 1 min). The major rod-mediated recovery phase immediately following the cone plateau showed a slope of −0.04 min$^{-1}$ (equivalent to a time constant of 650 s); recovery kinetics was ~7 times slower than normal (−0.3 ± 0.03 min$^{-1}$; 87 ~ 10 s). After ~5 h, rod-mediated thresholds reached normal values. The kinetics at two other loci in the patient were the same (data not shown). The heterozygote had normal rod function (Figs. 5A, 5C, and 5E).

### Cone vision when 11-cis-RDH activity is missing

Several previous findings have supported the hypothesis that the source of chromophore for cones may be in the retina (Rushton & Henry, 1968; Bunt-Milam & Saari, 1983; Das et al., 1992; Jin et al., 1994; Crouch et al., 1996). Considering this hypothesis and that 11-*cis*-RDH localizes to RPE, cone function may have been predicted to be normal in the absence of this enzyme activity. This was not the case in the homozygote with the *RDH5* null mutation. Cone ERG phototransduction activation was not normal (Fig. 5B). The maximum amplitude parameter was reduced in the homozygote ($R_{max}$ = 51 μV; normal = 83 ± 8 μV); sensitivity was normal ($\sigma$ = 2.0 log phot-td$^{-1}$ ·s$^{-3}$; normal = 2.28 ± 0.14 log phottd$^{-1}$·s$^{-3}$). There was also ~0.5 log unit elevation of L/M-cone psychophysical thresholds across most of the visual field; a parafoveal loss of ~2 log units was present (not shown). S-cone thresholds were undetectable in most of the field (not shown). The L/M-cone mediated portion of background adaptation

(Fig. 5D) showed a ~0.6 log unit elevation of $T_0$ parameter ($T_0$ = 5.2 log; $A_0$ = 0.7 log; $n$ = 0.75; normal, $T_0$ = 4.63 ± 0.22 log; $A_0$ = 0.77 ± 0.10 log; $n$ = 0.83 ± 0.04). These unexpected abnormalities would be explained by a retina-wide L/M-cone cell loss or reduction of outer segment length with a normal gain of L/M-cone activation.

Cone bleaching adaptation was markedly abnormal, showing the unusual feature of two L/M-cone phases. Following a full bleach, thresholds recovered rapidly to a transitory plateau and later recovered very slowly to the final cone plateau which was abnormally elevated by 2h(Fig. 5F). Normal cone recovery under these conditions is monophasic and complete within minutes. The homozygote's late slow L/M-cone recovery had a slope of $-0.02\ \text{min}^{-1}$ (1300 s) which was ~34 times slower than normal ($-0.68 \pm 0.09\ \text{min}^{-1}$ ; 38 ± 6 s). The heterozygote had normal L/M- and S-cone visual function (Figs. 5B, 5D, and 5F).

## Missing 11-cis-RDH activity does not preclude rapid recovery kinetics for rod and cone sensitivity

The unanticipated biphasic nature of L/M-cone recovery with strong bleaching lights in the homozygote (Fig. 5F) prompted further study of rod and cone dark-adaptation kinetics. This led to the finding that weak bleaches that selectively expose early portions of rod dark adaptation can be normal in this *RDH5* null mutant. In a representative normal, complete sensitivity recovery following 0.5% bleach takes ~10 min (Fig. 6A). This relatively slow recovery time would not be consistent with fast recoveries expected as a result of deactivation reactions or availability of free 11-*cis*-retinal in rod outer segments. Therefore we assume 0.5% bleach recovery requires regeneration. Recovery functions of the heterozygote (Fig. 6B) and the homozygote (Fig. 6C) following 0.5% bleach were indistinguishable from normal (Fig. 6D). Recovery of the rod-isolated ERG photoresponse following a 0.5% bleach was also normal in both subjects (not shown). These results suggest that the rate of chromophore production through the alternative red-ox pathway may be a dominant pathway following weak bleaches under normal physiological conditions. The kinetics of the rapid partial recovery observed in L/M-cone dark adaptation after a 99% bleach was superimposable with the recovery from 0.5% rod dark adaptation (Fig. 6D) suggesting chromophore may be provided rapidly through the alternative pathway to rods and cones. A limited supply of chromophore produced by the alternative pathway would explain the observed partial recovery following 99% cone bleach. Intermediate level bleaches provided further support for this idea.

Recovery of sensitivity following 2–13% bleaches in the homozygote were much slower than normal (Fig. 6C) suggesting necessity for the chromophore produced by 11-*cis*-RDH activity for normal recovery kinetics following lights bleaching >2% of rhodopsin. Similar to L/M-cone dark adaptation, there were rapid partial recoveries and plateaux (Cideciyan et al., 1997) during the early phase of each partial bleach rod dark-adaptation function (Fig. 6C). The kinetics of these rapid partial recovery functions after 2% and 3.5% bleaches were similar to the 0.5% recovery (Fig. 6D), further supporting the speculation that the alternative red-ox pathway is providing a limited supply of chromophore largely independent of bleached pigment.

Sensitivities to multispectral stimuli presented during the plateau periods [Fig. 6C (a–d)] provided direct evidence for rod-mediation (Fig. 6E). The plateau thresholds were strongly related to the fraction of rhodopsin bleached with a slope of 3.4 on double logarithmic coordinates (Fig. 6F). The plateau periods ended at ~20 min largely independent of the extent of bleach; the transitory cone plateau also ended at ~20 min (Fig. 5F). The rates of recovery following the plateaux were invariant among the partial bleaches and were the same as the recovery from the full bleach (Fig. 6C).

## Discussion

New complexity is added to the human visual cycle with the hypothesis that 11-*cis*-RDH activity does not account for all the retinoid dehydrogenase activity in the RPE (Saari et al., 2000). The present study advances this hypothesis through a number of *in vitro* and *in vivo* observations. We identified a novel disease-causing *RDH5* mutation in a family with fundus albipunctatus. This 11-*cis*-RDH mutant was shown to destabilize the enzyme structure and lead to inactivation. 11-*cis*-RDH was localized to the primate RPE. Our analyses with the use of a combination of cold and radioactive dinucleotides, NADPH and NADH, and competition assays showed another NADP/NADPH-specific red-ox system in RPE membranes capable of oxidizing 11-*cis*-retinol. *In vivo* results in the *RDH5* null mutant provided an opportunity to observe human visual function in the absence of 11-*cis*-RDH.

### Impact of the Arg157Trp RDH5 mutation on in vitro structure and function of 11-cis-RDH

The mutation described in this study results in a nonconservative replacement of Arg at codon 157 with Trp in the *RDH5* gene. A corresponding Arg in a homologous enzyme 17-β-HSD1 holds together the dinucleotide and steroid-binding domains by two critical hydrogen-bond interactions allowing efficient catalysis. The Trp substitution at Arg157 of 11-*cis*-RDH would be predicted to affect this interaction, destabilize proper folding of the bipartite structure of the enzyme, and lead to inactivation. Biochemical analyses indicated that the enzyme does not show residual activity even in the most favorable conditions and thus it is a null mutant. Our conclusions are supported by the finding that null mutations at Arg213 of the 11-β-HSD2 enzyme, corresponding to the Arg157 of 11-*cis*-RDH, cause hypertension (Rogoff et al., 1998). *In vitro* results in the Ser73Phe and Gly238Trp *RDH5* mutants (also associated with fundus albipunctatus) have previously shown 10–20% of wt activity (Yamamoto et al., 1999).

### How does the lack of 11-cis-RDH activity affect rods in vivo?

11-*cis*-RDH is not necessary for complete regeneration and normal light-triggered activation of rod outer segments. The early activation phase of rod phototransduction, as measured by the sensitivity parameter of the rod-isolated ERG photoresponse (Hood & Birch, 1994), was normal. Normal photoresponse maximum amplitude would also indicate normal length of rod outer segments (Hood & Birch, 1994); normal absolute rod sensitivity measured psychophysically across most of the retina would be consistent. 11-*cis*-RDH activity is also not necessary for the light adaptation of the human rod system as shown by the normal rise of rod thresholds on dim backgrounds that cause insignificant bleaching. This would be consistent with the current understanding of the molecular mechanisms of vertebrate light adaptation (Pugh et al., 1999).

A key finding of this study was that the rate of rod sensitivity recovery following a weak (0.5%) bleach in the homozygote was normal and thereby independent of 11-*cis*-RDH activity. There are three potential contributors to this recovery: deactivation reactions (e.g. phosphorylation by rhodopsin kinase and binding of arrestin), availability of free 11-*cis*-retinal in rod outer segments (Cocozza & Ostroy, 1987), and the activity of an alternative oxidation pathway. The first two possibilities would be expected to act on a time scale much shorter than the observed recovery lasting ~10 min. Thus, current results suggest the activity of the alternative oxidation pathway may play a significant role in the attainment of normal kinetics for visual sensitivity recovery following weak bleaches.

As anticipated, recovery of rod sensitivity following strong bleaches was much slower than normal. This slow recovery in the Arg157Trp *RDH5* homozygote cannot represent the retained partial activity of the mutant 11-*cis*-RDH, but it may represent the activity of the alternative

oxidation pathway. *RDH5* mutants with partial activity (as was postulated for the Ser73Phe and Gly238Trp mutations, Yamamoto et al., 1999) would be expected to show faster recovery than that shown in the current work. In a fundus albipunctatus patient of unknown genotype, a faster than expected pigment regeneration has been previously demonstrated (Margolis et al., 1987). Detailed and direct comparison of the visual consequences of the several different mutants now in the literature (Yamamoto et al., 1999; Gonzalez-Fernandez et al., 1999) should increase understanding of the relationship between retained 11-*cis*-RDH activity and visual function.

Sensitivity recovery following 97% bleach in the Arg157Trp *RDH5* homozygote could be described over a substantial range by a straight line on semilogarithmic coordinates (Lamb, 1990). Partial bleaches (2–13%) showed log-linear phases of recovery that matched the rate of recovery of the 97% bleach. These log-linear phases most likely are describing the time constant of the rate-limiting reaction in the alternative oxidation pathway. The identity of this rate-limiting reaction is difficult to predict, but it is of interest that the time constant resulting from a lack of 11-*cis*-RDH activity (~11 min) is similar to that resulting from a lack of rhodopsin kinase activity (~14 min) (Cideciyan et al., 1998). Such a result would be expected if the alternative oxidation pathway was using photolyzed chromophore as a substrate at later times after substantial bleaches and the reduction of the photolyzed chromophore was the rate-limiting reaction (Saari et al., 1998).

What could explain the dramatic and unexpected results of initial rapid recovery and transitory plateaux after partial bleaches in the homozygote? These early rapid recoveries could involve the alternative oxidation pathway that may be compartmentalized differently than *RDH5* in the RPE (Mata et al., 1998). Rate of recovery during the early phase could be limited by deactivation reactions in the rod outer segment and hydrolysis of 11-*cis*-retinyl esters and oxidation of 11-*cis*-retinol in the RPE. The plateaux may represent exhaustion of the immediate supply of the substrate for the alternative oxidation pathway.

To date, transitory sensitivity plateaux have only been found in two other retinopathies: Sorsby fundus dystrophy caused by mutations in the *TIMP3* gene and systemic vitamin A deficiency (Cideciyan et al., 1997). Both of these disorders are speculated to involve reduction of retinoid ester pool within the RPE (Cideciyan et al., 1997). The same *in vivo* physiological defect resulting from reduction of RPE esters and loss of 11-*cis*-RDH activity implies that the substrate for 11-*cis*-RDH activity may involve the retinoid ester pool in the RPE and not the photolyzed chromophore.

### Cone dysfunction is pronounced in a RDH5 null mutation

L/M-cone photoresponse maximum amplitude was reduced to 60% of normal and L/M-cone psychophysical sensitivities were reduced by 0.6 log units across most of the visual field. Dysfunction appeared to affect all three types cones as S-cone function of the homozygote was not detectable across most of the visual field. These data may be consistent with loss of cone outer segments, a stationary or possibly even a slowly progressive process. Alternatively, 11-*cis*-RDH activity may be necessary for complete regeneration of cone pigments (unlike that of rhodopsin) and the cone dysfunction in the homozygote is reflecting cones with partially regenerated pigment. It is of interest that fundus albipunctatus has been associated with maculopathy and widespread cone dystrophy in some patients of unknown genotype (Miyake et al., 1992). The patient in this study showed pronounced parafoveal cone (and rod) sensitivity loss that may be the functional equivalent of a bull's-eye lesion.

The major time constant of L/M-cone sensitivity recovery following a 99% bleach was ~22 min in the Arg157Trp *RDH5* mutant as compared to ~40 s in the normal. This dramatic result taken together with the localization of 11-*cis*-RDH to RPE cells (current work and Simon et

al., 1999) make a strong case that the RPE is likely the major source of chromophore to regenerate cone pigments following strong bleaches.

#### Acknowledgments

This research was supported by NIH (EY08061, EY05627, EY06935, and RR00166), Research to Prevent Blindness, Inc., Fight For Sight-Prevent Blindness America Research (GA99001), Foundation Fighting Blindness, Inc., the Mackall Trust, and E.K. Bishop Foundation. Clinical coordinator help was provided by Jiancheng Huang, Elaine DeCastro, and Joan Kim. UW41 antibody was prepared with the help of Mary Ann Asson-Batres, Janka Buczylko, John C. Saari, and John W. Crabb.

## References

BIRCH DG, HOOD DC, NUSINOWITZ S, PEPPERBERG DR. Abnormal activation and inactivation mechanisms of rod transduction in patients with autosomal dominant retinitis pigmentosa and the Pro-23-His mutation. Investigative Ophthalmology and Visual Science 1995;36:1603–1614. [PubMed: 7601641]

BOK D. The retinal pigment epithelium: A versatile partner in vision. Journal of Cell Science 1993;17:189–195.

BRETON R, HOUSEET D, MAZZA C, FONTECILLA-CAMPS JC. The structure of a complex of human 17beta-hydroxysteroid dehydrogenase with estradiol and NADP+ identifies two principal targets for the design of inhibitors. Structure 1996;4:905–916. [PubMed: 8805577]

BUNT-MILAM AH, SAARI JC. Immunocytochemical localization of two retinoid-binding proteins in vertebrate retina. Journal of Cell Biology 1983;97:703–712. [PubMed: 6350319]

CARR RE, RIPPS H, SIEGEL IM. Rhodopsin kinetics and rod adaptation in fundus albipunctatus. Documenta Ophthalmologica Proceedings Series 1974;4:193–204.

CIDECIYAN AV, JACOBSON SG. An alternative phototransduction model for human rod and cone ERG *a*-waves: Normal parameters and variation with age. Vision Research 1996;36:2609–2621. [PubMed: 8917821]

CIDECIYAN AV. *In vivo* assessment of photoreceptor function in human diseases caused by photoreceptor-specific gene mutations. Methods in Enzymology 2000;316:611–626. [PubMed: 10800705]

CIDECIYAN AV, LAMB TD, PUGH EN JR. HUANG Y, JACOBSON SG. Rod plateaux during dark adaptation in Sorsby's fundus dystrophy and vitamin A deficiency. Investigative Ophthalmology and Visual Science 1997;38:1786–1794. [PubMed: 9286267]

CIDECIYAN AV, ZHAO X, NIELSEN L, KHANI SC, JACOBSON SG, PALCZEWSKI K. Null mutation in the rhodopsin kinase gene slows recovery kinetics of rod and cone phototransduction in man. Proceedings of the National Academy of Sciences of the U.S.A 1998;95:328–333.

COCOZZA JD, OSTROY SE. Factors affecting the regeneration of rhodopsin in the isolated amphibian retina. Vision Research 1987;27:1085–1091. [PubMed: 3116765]

CROUCH RK, CHADER GJ, WIGGERT B, PEPPERBERG DR. Retinoids and the visual process. Photochemistry and Photobiology 1996;64:613–621. [PubMed: 8863467]

DAS SR, BHARDWAJ N, KJELDBYE H, GOURAS P. Muller cells of chicken retina synthesize 11-*cis*-retinol. Biochemical Journal 1992;285:907–913. [PubMed: 1497628]

DRIESSEN CAGG, WINKENS HJ, KUHLMANN ED, JANSSEN APM, VAN VUGT AHM, DEUTMAN AF, JANSSEN JJM. The visual cycle retinal dehydrogenase: Possible involvement in the 9-*cis* retinoic acid biosynthetic pathway. FEBS Letters 1998;428:135–140. [PubMed: 9654122]

GONZALEZ-FERNANDEZ F, KURZ D, BAO Y, NEWMAN S, CONWAY BP, YOUNG JE, HAN DP, KHANI SC. 11-*cis* Retinol dehydrogenase mutations as a major cause of the congenital night-blindness disorder known as fundus albipunctatus. Molecular Vision 1999;5:41. [PubMed: 10617778]

HOOD DC, BIRCH DG. Rod phototransduction in retinitis pigmentosa: Estimation and interpretation of parameters derived from the rod *a*-wave. Investigative Ophthalmology and Visual Science 1994;35:2948–2961. [PubMed: 8206712]

HOOD DC, GREENSTEIN V. Models of the normal and abnormal rod system. Vision Research 1990;30:51–68. [PubMed: 2321366]

JACOBSON SG, VOIGT WJ, PAREL J-M, APATHY PP, NGHIEM-PHU L, MYERS SW, PATELLA VM. Automated light- and dark-adapted perimetry for evaluating retinitis pigmentosa. Ophthalmology 1986;93:1604–1611. [PubMed: 3808619]

JIN JG, JONES J, CORNWALL MC. Movement of retinal along cone and rod photoreceptors. Visual Neuroscience 1994;11:389–399. [PubMed: 8003460]

JORNVALL H, PERSSON B, KROOK M, ATRIAN S, GONZALEZ-DUARTE R, JEFFERY J, GHOSH D. Short-chain dehydrogenases/reductases (SDR). Biochemistry 1995;34:6003–6013. [PubMed: 7742302]

LAMB, TD. Dark adaptation: A re-examination. In: HESS, RF.; SHARPE, LT.; NORDBY, K., editors. Night Vision. Cambridge University Press; New York: 1990. p. 177-222.

LION F, ROTMANS JP, DAEMEN FJM, BONTING SL. Biochemical aspects of the visual process. XXVII. Stereospecificity of ocular retinal dehydrogenases and the visual cycle. Biochimica et Biophysica Acta 1975;384:283–292. [PubMed: 1125252]

MARGOLIS S, SIEGEL IM, RIPPS H. Variable expressivity in fundus albipunctatus. Ophthalmology 1987;94:1416–1422. [PubMed: 3500444]

MARMOR MF. Fundus albipunctatus: A clinical study of the fundus lesions, the physiologic deficit, and the vitamin A metabolism. Documenta Ophthalmologica 1977;43:277–302. [PubMed: 302784]

MARMOR MF. Long-term follow-up of the physiologic abnormalities and fundus changes in fundus albipunctatus. Ophthalmology 1990;97:380–384. [PubMed: 2336278]

MATA NL, TSIN AT. Distribution of 11-*cis* LRAT, 11-*cis* RD and 11-*cis* REH in bovine retinal pigment epithelium membranes. Biochimica et Biophysica Acta 1998;1394:16–22. [PubMed: 9767084]

MATA NL, VILLAZANA ET, TSIN ATC. Colocalization of 11-*cis* retinyl esters and retinyl ester hydrolase activity in retinal pigment epithelium plasma membrane. Investigative Ophthalmology and Visual Science 1998;39:1312–1319. [PubMed: 9660478]

MIYAKE Y, SHIROYAMA N, SUGITA S, HORIGUCHI M, YAGASAKI K. Fundus albipunctatus associated with cone dystrophy. British Journal of Ophthalmology 1992;76:375–379. [PubMed: 1622952]

OTTO-BRUC A, FARISS RN, HAESELEER F, HUANG J, BUCZYLKO J, SURGUCHEVA I, BAEHR W, MILAM AH, PALCZEWSKI K. Localization of guanylate cyclase-activating protein 2 in mammalian retinas. Proceedings of the National Academy of Sciences of the U.S.A 1997;94:4727–4732.

PALCZEWSKI K, BUCZYLKO J, LEBIODA L, CRABB JW, POLANS AS. Identification of the N-terminal region in rhodopsin kinase involved in its interaction with rhodopsin. Journal of Biological Chemistry 1993;268:6004–6013. [PubMed: 8383684]

PALCZEWSKI K, SAARI JC. Activation and inactivation steps in the visual transduction pathway. Current Opinion in Neurobiology 1997;7:500–504. [PubMed: 9287193]

PEARSON WR, LIPMAN DJ. Improved tools for biological sequence comparison. Proceedings of the National Academy of Sciences of the U.S.A 1988;85:2444–2468.

PUGH EN JR. NIKONOV S, LAMB TD. Molecular mechanisms of vertebrate photoreceptor light adaptation. Current Opinion in Neurobiology 1999;9:410–418. [PubMed: 10448166]

RING CS, COHEN FE. Modeling protein structures: Construction and their applications. FASEB Journal 1993;7:783–790. [PubMed: 8330685]

ROGOFF D, SMOLENICKA Z, BERGADA I, VALLEJO G, BARONTINI M, HEINRICH JJ, FERRARI P. The codon 213 of the 11beta-hydroxysteroid dehydrogenase type 2 gene is a hot spot for mutations in apparent mineralocorticoid excess. Journal of Clinical Endocrinology and Metabolism 1998;83:4391–4393. [PubMed: 9851783]

RUSHTON WA, HENRY GH. Bleaching and regeneration of cone pigments in man. Vision Research 1968;8:617–631. [PubMed: 5729910]

SAARI JC, BREDBERG DL. Acyl-CoA:retinal acyltransferase and lecithin:retinal acyltransferase activities of bovine retinal pigment epithelial microsomes. Methods in Enzymology 1990;190:156–163. [PubMed: 2087167]

SAARI JC, BREDBERG DL, GARWIN GG, WHEELER T, PALCZEWSKI K. Assays of retinoid dehydrogenases by phase partition. Analytical Biochemistry 1993;213:128–132. [PubMed: 8238865]

SAARI JC, GARWIN GG, HAESELEER F, JANG G-F, PALCZEWSKI K. Phase partition and high-performance liquid chromatography assays of retinoid dehydrogenases. Methods in Enzymology 2000;316:359–371. [PubMed: 10800687]

SAARI JC, GARWIN GG, VAN HOOSER JP, PALCZEWSKI K. Reduction of all-*trans*-retinal limits regeneration of visual pigment in mice. Vision Research 1998;38:1325–1333. [PubMed: 9667000]

SIMON A, HELLMAN U, WERNSTEDT C, ERIKSSON U. The retinal pigment epithelial-specific 11-*cis* retinal dehydrogenase belongs to the family of short chain alcohol dehydrogenases. Journal of Biological Chemistry 1995;270:1107–1112. [PubMed: 7836368]

SIMON A, ROMERT A, GUSTAFSON A-L, MCCAFFERY JM, ERIKSSON U. Intracellular localization and membrane topology of 11-*cis* retinal dehydrogenase in the retinal pigment epithelium suggest a compartmentalized synthesis of 11-*cis* retinaldehyde. Journal of Cell Science 1999;112:549–558. [PubMed: 9914166]

SUZUKI Y, ISHIGURO S-I, TAMAI M. Identification and immunohistochemistry of retinal dehydrogenase from bovine retinal pigment epithelium. Biochimica et Biophysica Acta 1993;1163:201–208. [PubMed: 8490052]

YAMAMOTO H, SIMON A, ERIKSSON U, HARRIS E, BERSON EL, DRYJA TP. Mutations in the gene encoding 11-*cis* retinal dehydrogenase cause delayed dark adaptation and fundus albipunctatus. Nature Genetics 1999;22:188–191. [PubMed: 10369264]

ZIMMERMAN WF. Subcellular distribution of 11-*cis*-retinol dehydrogenase activity in bovine pigment epithelium. Experimental Eye Research 1976;23:159–164. [PubMed: 976365]

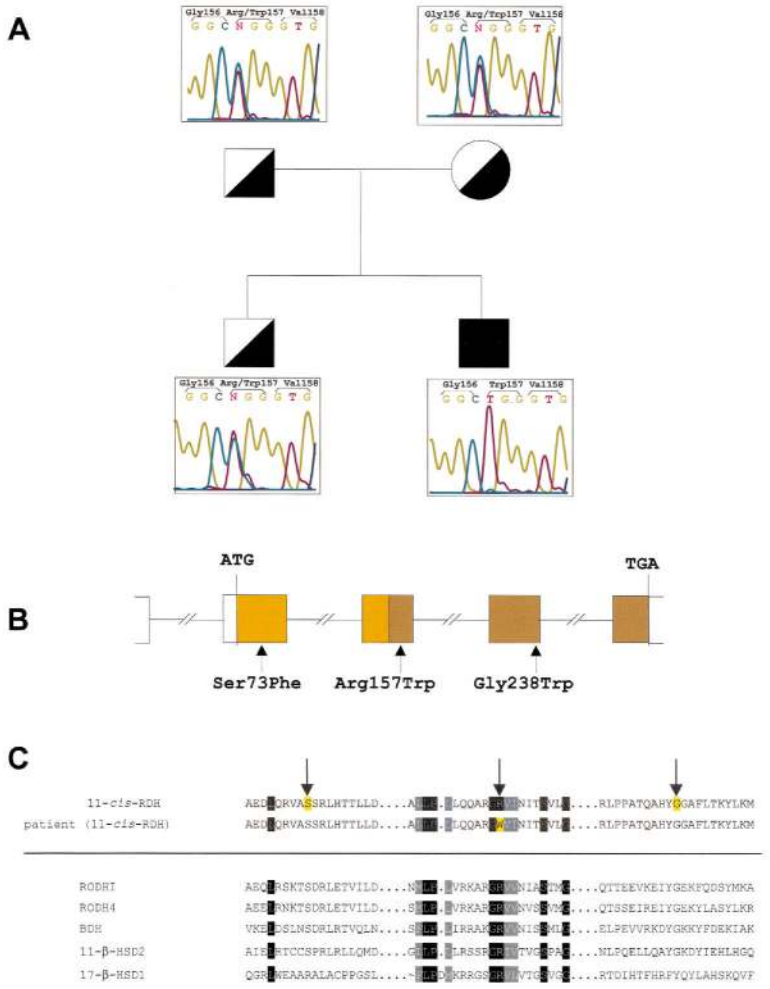


**Fig. 1.**

Segregation of mutations in the *RDH5* gene in a family and position of missense mutations. (A) Identification of a missense mutation (CGG→TGG) in exon 3 at codon 157 (Arg157Trp). (B) Exon-intron organization of the *RDH5* gene. Orange boxes cover the cofactor binding domain. The active domain is shaded in brown. Mutations in the current and previous work (Yamamoto et al., 1999) are indicated. (C) Amino acid sequence alignment of regions encompassing the mutations in 11-*cis*-RDH and related proteins. Strictly conserved amino acids are shown in white letters on black background. The conservative substitutions are shown in white letters on gray background. The mutated residues are shaded in yellow and indicated by arrows.

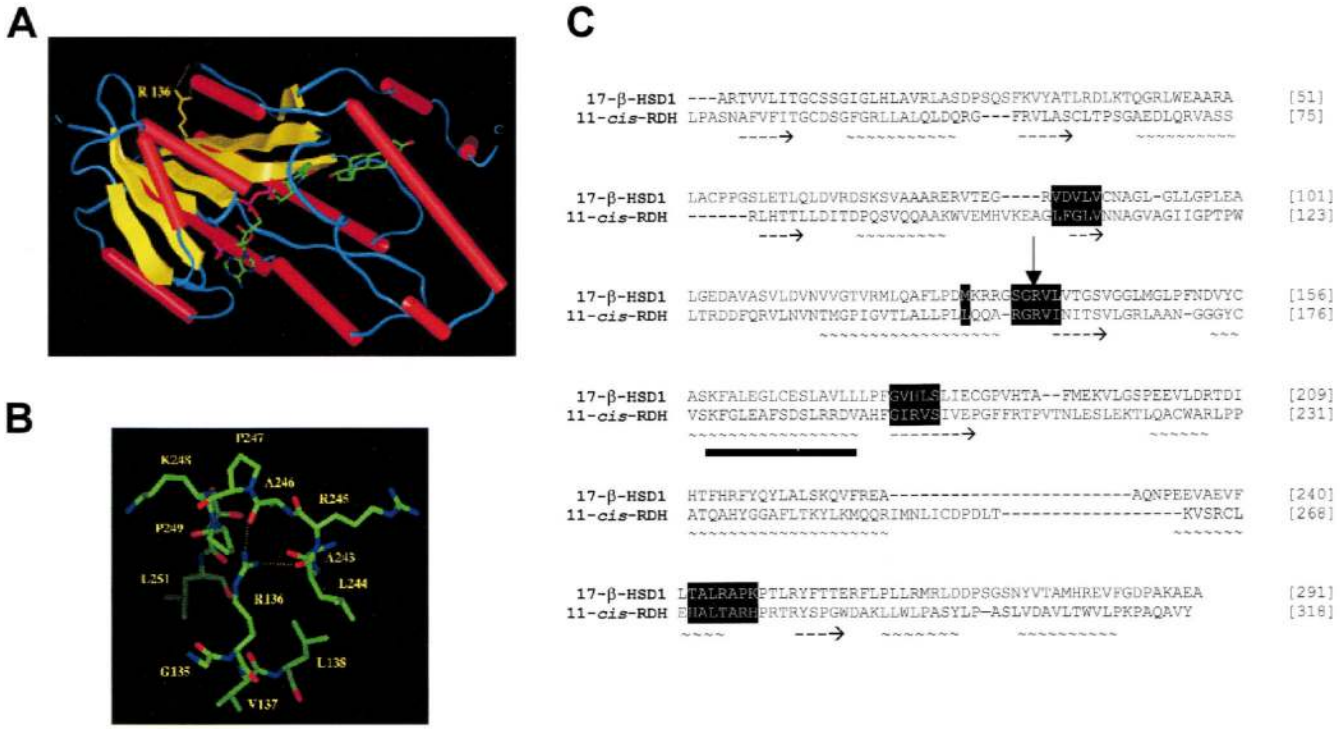


**Fig. 2.**

Structural model of 11-*cis*-RDH. (A) Model of 11-*cis*-RDH based on the crystal structure of 17-β-hydroxysteroid dehydrogenase (17-β-HSD1) around Arg136 with bound estradiol and NADP (Breton et al., 1996). Note that Arg136 corresponds to Arg157 in 11-*cis*-RDH. (B) Expanded view around Arg136. (C) Sequence alignment of 17-β-HSD1 and 11-*cis*-RDH. Marked residues (white letters on the black background) are located within 7Å of Arg136. Symbols: –, β-strand; and ~~~~, α-helical region. The black box represents the antibody epitope of UW41.

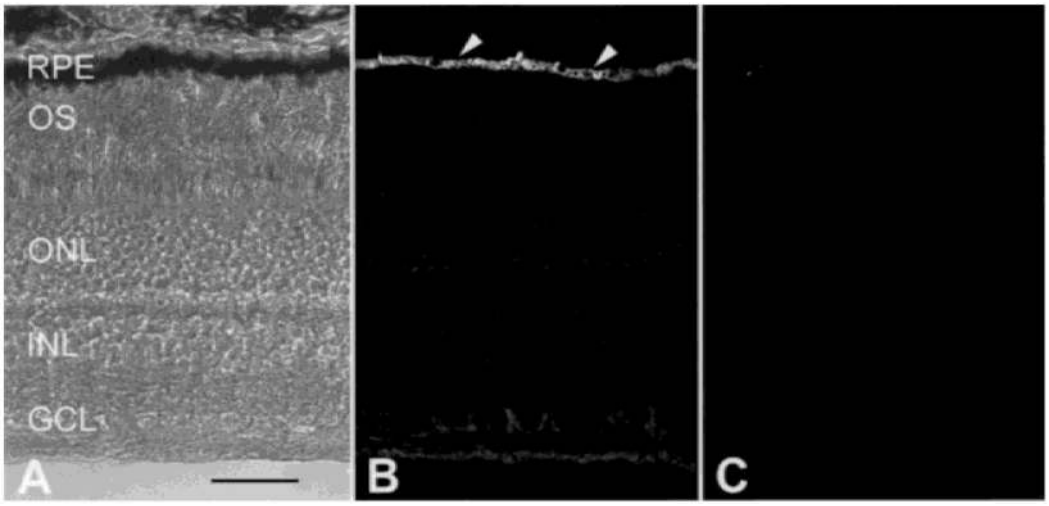


**Fig. 3.**

Immunolocalization of 11-*cis*-RDH. (A) DIC image of an unstained cryosection of monkey retina showing the location of RPE and layers of the neural retina. (B) 11-*cis*-RDH immunolabeling (UW40 polyclonal antibody) in monkey retina. Arrowheads denote the RPE, which is intensely immunopositive. With the exception of a very faint fluorescent signal in the GCL, the neural retina is not immunolabeled. (C) Immunolabeling of the RPE is abolished in sections of monkey retina incubated in UW40 antisera preadsorbed with the 11-*cis*-RDH peptide SKFGLEAFSDSLRRDV. Magnification bar = 50 μm. OS: outer segment layer; ONL: outer nuclear layer; INL: inner nuclear layer, and GCL: ganglion cell layer.

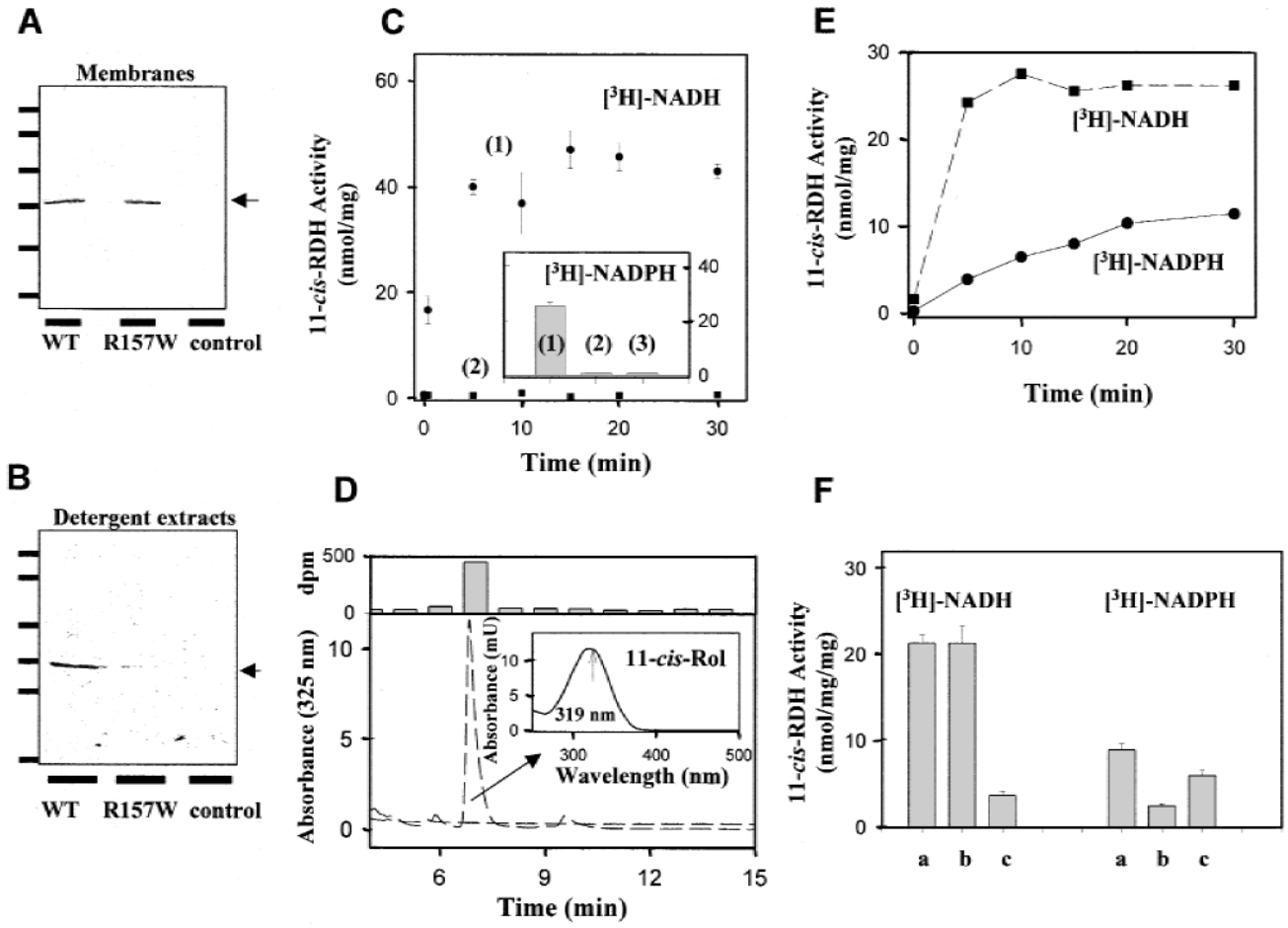


**Fig. 4.**

Functional characterization of recombinant wild-type and Arg157Trp mutant of 11-*cis*-RDH expressed in insect cells. (A) Equal amounts of membranous fractions of SF9 cells were analyzed employing immunoblotting for the expression levels of wild-type (wt) and Arg157Trp mutant of 11-*cis*-RDH probed with UW41. (B) Immunoblot analysis of proteins solubilized with 10 mM Chaps in 10 mM BTP, pH 7.5 from membranous fractions of SF9 cells expressing wt and Arg157Trp mutant of 11-*cis*-RDH. (A,B) Arrows represent bands corresponding to 11-*cis*-RDH. (C) Time course of 11-*cis*-retinal reduction by wt (closed circles) and Arg157Trp mutant (closed squares) of 11-*cis*-RDH. The 11-*cis*-RDH activity was tested using 11-*cis*-retinal as substrate and [$^3$H]-NADH. Both proteins were expressed in SF9 insect cells in roughly equal amounts as shown in panel A. The membrane suspensions from SF9 cells were used in the assays. *Inset*. Activity of wt (1) and Arg157Trp mutant of 11-*cis*-RDH (2) and control uninfected SF9 cell membranes (3) using 11-*cis*-retinal and [$^3$H]-NADPH as cofactor for 10 min. (D) Identification of 11-*cis*-retinol as a product of 11-*cis*-retinal reduction in reaction catalyzed by 11-*cis*-RDH. [$^3$H]-11-*cis*-retinol was identified by co-elution with an authentic 11-*cis*-retinol standard employing normal phase HPLC separation (main panel for absorption profile, and upper panel for the radioactivity profile), and by characteristic UV-Vis spectrum with λ maximum at 319 nm (inset panel). (E) Time course of 11-*cis*-retinal reduction by RPE microsomes. The 11-*cis*-RDH activity was tested using 11-*cis*-retinal and [$^3$H]-NADH or [$^3$H]-NADPH. (F) Competition of NADH or NADPH with [$^3$H] NADH or [$^3$H] NADPH in 11-*cis*-RDH activity assays using RPE microsomes. 11-*cis*-RDH activity was tested at 30 °C

for 10 min using 10 μM [$^3$H]-NADH or [$^3$H]-NADPH (a), in the presence of 200 μM NADPH (b), or 200 μM NADH (c).

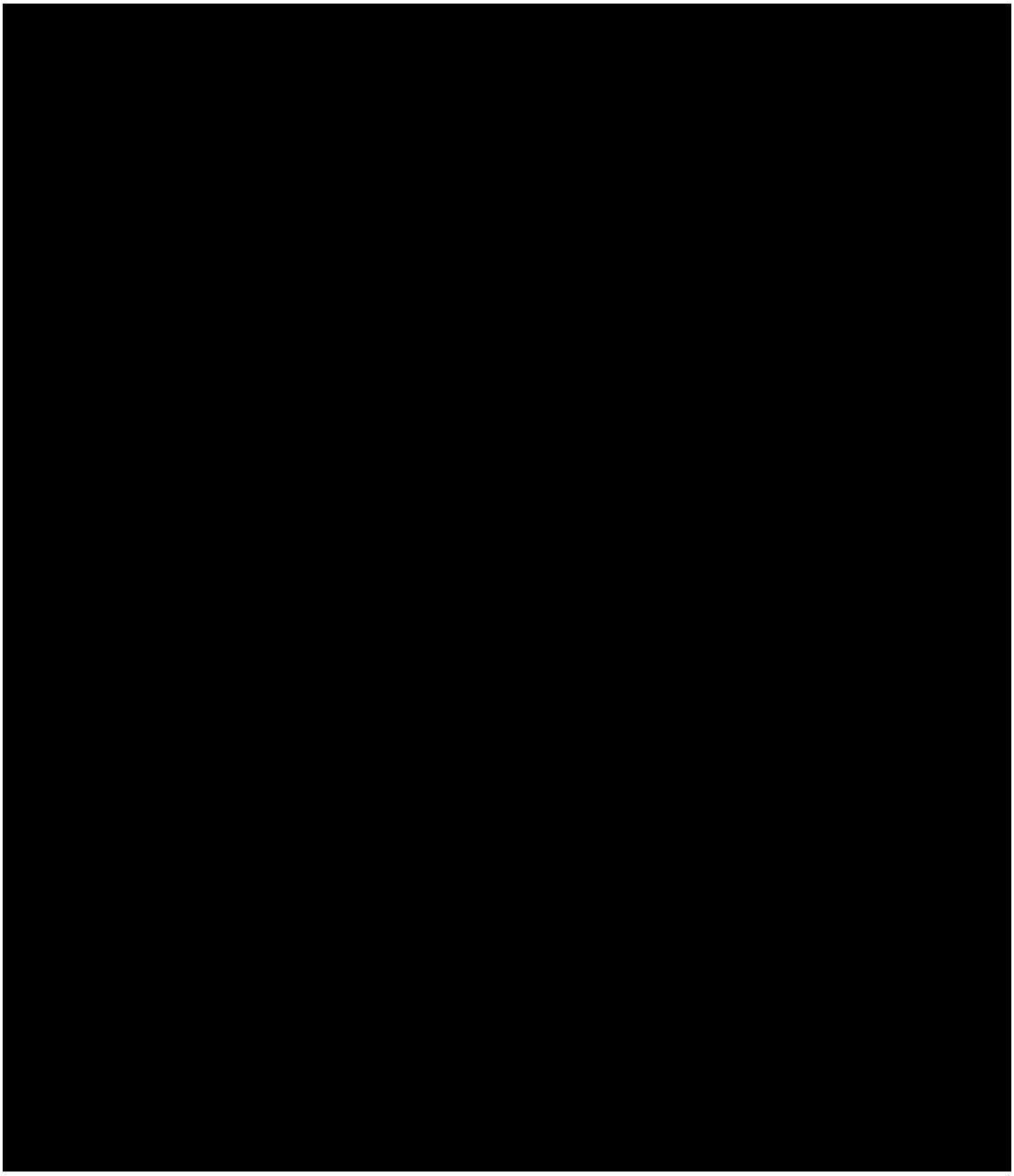

**Fig. 5.**

Activation kinetics and adaptation. Rod- (A) and cone-isolated (B) ERG photoresponses representing phototransduction activation in the homozygote and the heterozygote evoked by 4.6 log scot-td.s blue (A) and 4.1 log phot-td.s red stimuli (B). Lines show the fit to a model for activation of phototransduction. Arrows along the ordinate denote lower limit (mean − 2 S.D) of photoresponse maximum amplitude. Rod- (C,E) and cone-mediated (D,F) thresholds either on increasing background intensities (C,D) or following a full bleach (E,F) are shown for the homozygote, heterozygote, and a representative normal subject at 12 deg inferior field with 500-nm (C,E) or 650-nm (D,F) stimuli. A model of background adaptation is fit to the data (C,D). DA is dark-adapted. Slopes of the major log–linear sensitivity recovery kinetics are shown (E,F gray lines).

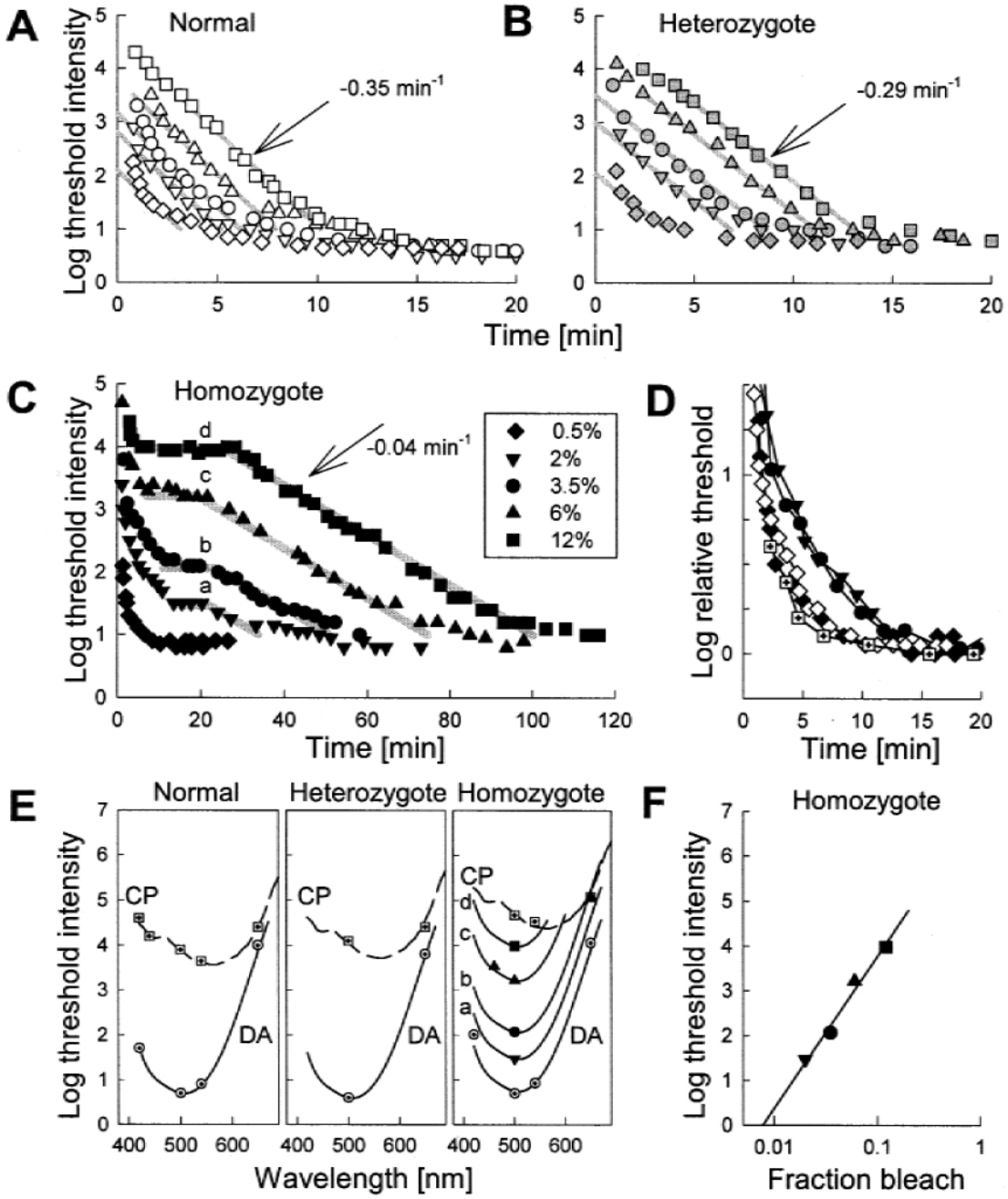


**Fig. 6.**

Rod plateaux after partial bleaches. Thresholds to 500-nm stimuli at 12 deg inferior field following various flash bleaches are shown for a normal subject (A), the heterozygote (B), and the homozygote (C). Gray parallel lines are simultaneously fit to the log–linear recovery portions of the partial bleaches and the full bleach data shown in Fig. 4. In the homozygote (C), gray diagonal lines are extended with horizontal lines corresponding to the plateau regions (a–d). Kinetics of the early rapid rod sensitivity recovery following 0.5%, 2%, and 3.5% bleaches in the homozygote are compared to the 99% cone recovery in the homozygote (squares with cross) and the 0.5% rod recovery of the normal (D). All curves are vertically shifted to match thresholds at 20 min. Thresholds obtained with different wavelength stimuli dark-

adapted (DA) during the cone plateau (CP) following a full bleach in the normal, heterozygote, and homozygote are compared to thresholds during rod plateaux (a–d) following partial bleaches in the homozygote (E). Scotopic luminous efficiency function (solid lines) and the peripheral cone spectral-sensitivity function (dashed lines) are fit to the available thresholds. Rod plateau thresholds of the homozygote plotted against fraction of bleach (F).